Clouds and the Earth's Radiant Energy System (CERES): Algorithm Overview

Bruce A. Wielicki, Bruce R. Barkstrom, Bryan A. Baum, Thomas P. Charlock, Richard N. Green,
David P. Kratz, Robert B. Lee, III, Patrick Minnis, G. Louis Smith, Takmeng Wong, David F. Young,
Robert D. Cess, James A. Coakley, Jr., Dominique A. H. Crommelynck, Leo Donner,
Robert Kandel, Michael D. King, Alvin J. Miller, Veerabhadran Ramanathan,
David A. Randall, Larry L. Stowe, and Ronald M. Welch

Abstract— The Clouds and the Earth's Radiant Energy System (CERES) is part of NASA's Earth Observing System (EOS). CERES objectives include the following.

1) For climate change analysis, provide a continuation of the Earth Radiation Budget Experiment (ERBE) record of radiative fluxes at the top-of-the-atmosphere (TOA), analyzed using the same techniques as the existing ERBE data.
2) Double the accuracy of estimates of radiative fluxes at TOA and the earth's surface;
3) Provide the first long-term global estimates of the radiative fluxes within the earth's atmosphere.
4) Provide cloud property estimates collocated in space and time that are consistent with the radiative fluxes from surface to TOA.

In order to accomplish these goals, CERES uses data from a combination of spaceborne instruments: CERES scanners, which are an improved version of the ERBE broadband radiometers, and collocated cloud spectral imager data on the same spacecraft. The CERES cloud and radiative flux data products should prove extremely useful in advancing the understanding of cloud-radiation interactions, particularly cloud feedback effects on the earth's radiation balance. For this reason, the CERES data should be fundamental to our ability to understand, detect, and predict global climate change. CERES results should also be very useful for studying regional climate changes associated with deforestation, desertification, anthropogenic aerosols, and El Niño/Southern Oscillation events.

This overview summarizes the Release 2 version of the planned CERES data products and data analysis algorithms. These algorithms are a prototype for the system that will produce the scientific data required for studying the role of clouds and radiation in the earth's climate system. This release will produce a data processing system designed to analyze the first CERES data, planned for launch on Tropical Rainfall Measuring Mission (TRMM) in November 1997, followed by the EOS morning (EOS-AM1) platform in 1998.

Index Terms—Algorithms, clouds, meteorology, radiation monitoring.

B. A. Wielicki, B. R. Barkstrom, B. A. Baum, T. P. Charlock, R. N. Green, D. P. Kratz, R. B. Lee, III, P. Minnis, T. Wong, and D. F. Young are with the Atmospheric Sciences Division, NASA Langley Research Center, Hampton, VA 23681-0001 USA (e-mail: b.a.wielicki@larc.nasa.gov).

G. L. Smith is with the Virginia Polytechnic Institute and State University, Blacksburg, VA 24061-0238 USA.

R. D. Cess is with the State University of New York at Stony Brook, Stony Brook, NY 11790 USA.

J. A. Coakley, Jr., is with Oregon State University, Corvallis, OR 97331 USA.

D. A. H. Crommelynck is with the Institut Royal Meteorologique, B-1180 Brussels, Belgium.

L. Donner is with the National Oceanic and Atmospheric Administration/Geophysical Fluid Dynamics Laboratory, Princeton, NJ 08542 USA.

R. Kandel is with the Laboratoire de Meteorologie Dynamique, Ecole Polytechnique, 91128 Palaiseau, France.

M. D. King is with NASA's Goddard Space Flight Center, Greenbelt, MD 20771 USA.

A. J. Miller is with the National Oceanic and Atmospheric Administration NWS/National Center for Environmental Prediction, Camp Springs, MD 20233 USA.

V. Ramanathan is with the Scripps Institution of Oceanography, University of California, San Diego, La Jolla, CA 92093-0237 USA.

D. A. Randall is with Colorado State University, Fort Collins, CO 80521 USA.

L. L. Stowe is with the National Oceanic and Atmospheric Administration/National Environmental Satellite Data and Information Service, Washington, DC 20233 USA.

R. M. Welch is with the University of Alabama-Huntsville, Huntsville, AL 35807 USA.

Publisher Item Identifier S 0196-2892(98)04158-8.

I. INTRODUCTION

THE PURPOSE of this overview is to provide a brief summary of the Clouds and the Earth's Radiant Energy System (CERES) science objectives, historical perspective, algorithm design, and relationship to other Earth Observing System (EOS) instruments as well as important field experiments required for validation of the CERES results. The overview is designed for readers familiar with the Earth Radiation Budget Experiment (ERBE) and the International Satellite Cloud Climatology Project (ISCCP) data. For other readers, additional information on these projects can be found in many references [1], [2], [42], [43]. Given this background, many of the comments in this overview will introduce CERES concepts by comparison to the existing ERBE and ISCCP state-of-the-art global measurements of radiation budget and cloud properties. The overview will not be complete or exhaustive, but rather selective and illustrative. More complete descriptions are found in the CERES Algorithm Theoretical Basis Documents (ATBD's) (http://eospso.gsfc.nasa.gov/atbd/cerestables.html), and they

are referenced where appropriate. The overview as well as the entire set of ATBD's that constitute the CERES design are the product of the entire CERES Science Team and the CERES Data Management Team. We have simply summarized that much larger set of documentation in this document.

Scientific Objectives: The scientific justification for the CERES measurements can be summarized by the following three assertions.

1) Changes in the radiative energy balance of the earth-atmosphere system can cause long-term climate changes, including a carbon dioxide induced "global warming."

2) Besides the systematic diurnal and seasonal cycles of solar insolation, changes in cloud properties, including amount, height, and optical thickness, cause the largest changes in the earth's radiative energy balance.

3) Cloud physics is one of the weakest components of current climate models used to predict potential global climate change.

The 1990 Intergovernmental Panel on Climate Change (IPCC) assessment of the uncertainty of the prediction of potential future global climate change [25] concluded that "the radiative effects of clouds and related processes continue to be the major source of uncertainty." The United States Global Change Research Program (USGCRP) classified the role of clouds and radiation as its highest scientific priority [7]. There are many excellent summaries of the scientific issues [23], [26], [40], [41], [55] concerning the role of clouds and radiation in the climate system. These issues naturally lead to a requirement for improved global observations of both radiative fluxes and cloud physical properties. The CERES Science Team, in conjunction with the EOS Investigators Working Group, representing a wide range of scientific disciplines from oceans to land processes to atmosphere, has examined these issues and proposed an observational system with the following objectives.

1) For climate change analysis, provide a continuation of the ERBE record of radiative fluxes at the top-of-the-atmosphere (TOA), using CERES data analyzed with the same algorithms that produced the ERBE data.

2) Double the accuracy of estimates of radiative fluxes at the TOA and earth's surface.

3) Provide the first long-term global estimates of the radiative fluxes within the earth's atmosphere.

4) Provide cloud property estimates that are consistent with the radiative fluxes from surface to TOA.

The most recent IPCC assessment of climate change [26] concludes that the remaining uncertainties include "feedbacks associated with clouds" and "systematic collection of long-term instrumental and proxy observations of the climate system variables (e.g., solar output, atmospheric energy balance components, ...)" The long-term CERES measurements target both of these needs.

The CERES ATBD's provide a technical plan for accomplishing these scientific objectives. The ATBD's include detailed specification of data products as well as the algorithms used to produce those products. CERES vali-

dation plans are provided in a separate set of documents (http://eospso.gsfc.nasa.gov/validation/valplans.html).

II. HISTORICAL PERSPECTIVE

We will briefly outline the CERES planned capabilities and improvements by comparison to the existing ERBE, ISCCP, and Surface Radiation Budget (SRB) projects. A schematic of radiative fluxes and cloud properties as produced by ERBE, SRB, and ISCCP, as well as those planned for CERES are illustrated in Fig. 1. Key changes in the CERES retrievals as compared to ERBE and SRB include the following.

1) Scene Identification:

a) ERBE measured only TOA fluxes [1], [2] and used only ERBE broadband radiance data, even for the difficult task of identifying each ERBE field-of-view (FOV) as cloudy or clear [54]. CERES will identify clouds using collocated high-spectral and spatial resolution cloud imager radiance data from the same spacecraft as the CERES broadband radiance data. CERES will use the Visible Infrared Scanner (VIRS) on the Tropical Rainfall Measuring Mission (TRMM), launched in November 1997. VIRS is a slightly advanced instrument similar to Advanced Very High Resolution Radiometer (AVHRR), but which has higher spatial resolution (2 km), adds a 1.6-μm channel for improved cloud microphysics and aerosols, and has a deployable solar diffuser plate to monitor long-term instrument gain stability. CERES will use the Moderate Resolution Imaging SpectroRadiometer (MODIS) on EOS morning (EOS-AM1) and evening (EOS-PM1) platforms. MODIS [28] is a major improvement over AVHRR, with spatial resolutions varying from 250 m to 1 km, several additional cloud remote-sensing spectral channels (see Section III-E3 for details), and greatly improved solar spectral channel calibration, including the ability to use the lunar surface as a stability calibration target.

b) ERBE only estimated cloud properties as one of four cloud amount classes [54]. CERES will identify clouds by cloud amount, height, optical depth, and cloud particle size and phase. CERES will also classify scenes as single or multilayered. The differences in cloud property identification for ISCCP, ERBE, and CERES are shown at the bottom of Fig. 1. For example, ERBE had no scene identification for cloud height, optical depth, or cloud particle size.

2) Angular Sampling:

a) ERBE used empirical anisotropic models that were only a function of cloud amount and four surface types [49]. This left significant rms and bias errors in TOA fluxes [50]. CERES will fly a new rotating azimuth plane (RAP) scanner to sample radiation across the entire hemisphere of scattered and emitted broadband radiation. The CERES RAP scanner data will be merged with coincident cloud imager-derived cloud physical and radiative properties to develop a more complete set of models of the radiative anisotropy of shortwave (SW) and longwave (LW) radiation.
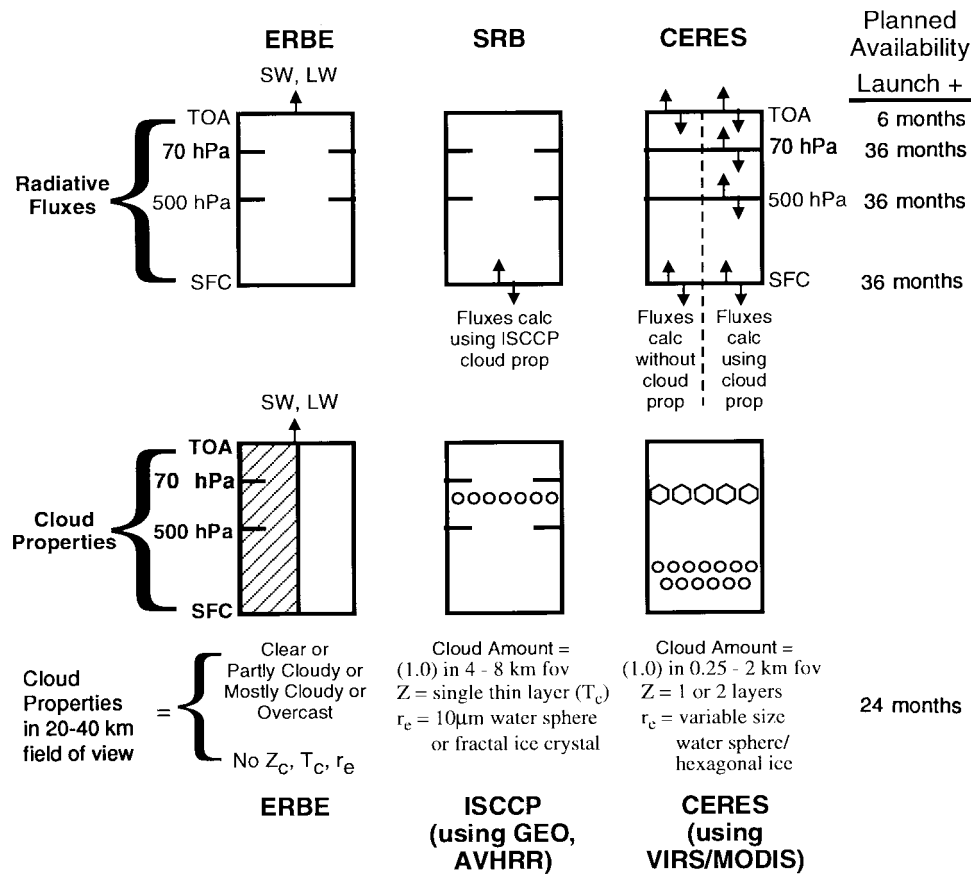
Fig. 1. Top: compares radiative fluxes derived by ERBE, SRB, and CERES. Bottom: compares cloud amount and layering assumptions used by ERBE, ISCCP, and CERES.

Greatly improved TOA flux accuracies should be possible [56].

3) Time Sampling:

a) ERBE used a time-averaging strategy that relied only on the broadband ERBE data and used other data sources only for validation and regional case studies [5]. CERES will use the three-hourly geostationary (GEO) satellite data of ISCCP to aid in time interpolation of TOA fluxes between CERES observation times [58]. Calibration problems with the narrowband ISCCP data (see [29]) will be eliminated by adjusting the data to agree at the CERES observation times. In this sense, the narrowband data are used to provide a diurnal cycle perturbation to the mean radiation fields.

4) Surface and In-Atmosphere Radiative Fluxes:

a) SRB uses ISCCP-determined cloud properties [38], [42], [43], [53] and calibration to estimate surface fluxes. CERES will provide two types of surface fluxes: 1) a set based on an attempt to directly relate CERES TOA fluxes to surface fluxes (see [8], [27], and [32]) and 2) a set based on the best information on cloud, surface, and atmosphere properties that are used to calculate surface fluxes, while constraining the radiative model solution to agree with CERES TOA flux observations [10]. These calculations are first performed at the CERES field of view scale (20 km at nadir) to minimize problems caused by the nonlinear

relationship between cloud physical properties and radiative fluxes.

b) Radiative fluxes within the atmosphere will be estimated using the same radiative model solution used to obtain the surface fluxes, and they will initially be provided at 500 hPa (midtroposphere) and 70 hPa (lower stratosphere). Later, radiative flux estimates at 4–12 additional levels in the troposphere are planned, with the number of tropospheric levels dependent on the results of postlaunch validation studies.

III. CERES ALGORITHM SUMMARY

A. Data Flow Diagram

The simplest way to understand the structure of the CERES data analysis algorithms is to examine the CERES data flow diagram shown in Fig. 2. Circles in the diagram represent algorithm processes that are formally called subsystems. Subsystems are a logical collection of algorithms that together convert input data products into output data products. Boxes represent archival data products. Boxes with arrows entering a circle are input data sources for the subsystem, while boxes with arrows exiting the circles are output data products. Data output from the subsystems fall into the following three major types of archival products.

1) ERBE-like products, which are as identical as possible to the data products produced by ERBE. These products are used for climate monitoring and climate change studies.
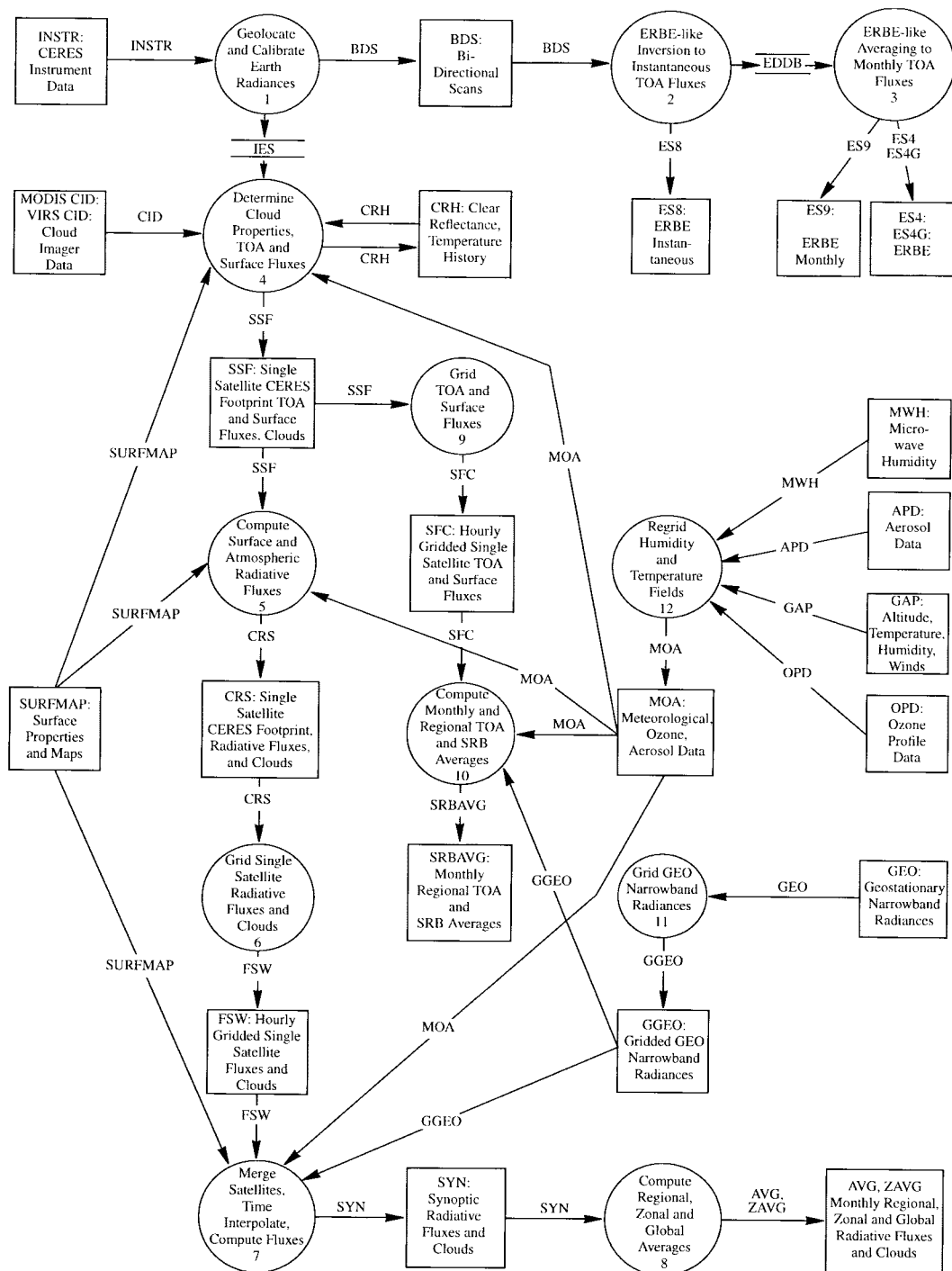
Fig. 2.   CERES data flow diagram. Boxes represent input or output archived data products. Circles represent algorithm processes.

They extend as consistently as possible the ERBE TOA flux climate record.

2) SURFACE products, which use cloud imager data for scene classification and new CERES-derived angular models to provide TOA fluxes with improved accuracy over those provided by the ERBE-like products. Direct relationships between surface fluxes and TOA fluxes are used where possible to construct SRB estimates that are as independent as possible of radiative transfer model assumptions. These surface flux estimates can be tuned directly to surface radiation measurements, such as

those from the international Baseline Surface Radiation Network (BSRN). These products are used for studies of land and ocean surface energy budget as well as climate studies that require higher accuracy TOA fluxes than those provided by the ERBE-like products.

3) ATMOSPHERE products, which use cloud-imager-derived cloud physical properties, National Centers for Environmental Prediction (NCEP) or EOS Data Assimilation Office (DAO) temperature and moisture fields, satellite measured ozone and aerosol data, CERES observed surface radiative properties, and a broadband

radiative transfer model to compute estimates of the upward and downward SW and LW radiative fluxes at the surface, selected levels within the atmosphere, and the TOA. By adjusting the most uncertain surface and cloud properties, the calculations are constrained to agree with the CERES TOA-measured fluxes, thereby producing an internally consistent data set of radiative fluxes and cloud properties. These products are designed for studies of energy balance within the atmosphere as well as climate studies that require consistent cloud, TOA, and surface radiation data sets. Data volume is much larger than for the ERBE-like and Surface data products.

The data flow diagram and the associated ATBD's are a work in progress. They represent the current understanding of the CERES Science Team and the CERES Data Management Team. The ATBD's are meant to change with time. To manage this evolution, the data products and algorithms will be developed in four releases or versions.

Release 1 (1996) was the initial prototype system. Release 1 was sufficiently complete to allow testing on existing global satellite data from ERBE, AVHRR, and High-Resolution Infrared Sounder (HIRS) instruments for October 1986 on NOAA-9. This release provided estimates of the computational resources required to process the CERES data as well as sensitivity studies of initial algorithm performance for global conditions.

Release 2 (1997) is the first operational system. It is designed using the experience from Release 1 and used to process the first CERES data following the November 28, 1997, launch of the TRMM.

Release 3 (1998) adds the capability to analyze MODIS radiance data to provide cloud properties. Release 3 will be used to process initial data from the EOS-AM1 platform planned for launch in June 1998 as well as EOS-PM1 planned for launch in December 2000.

Release 4 (2001) is planned for three years after the launch of the EOS-AM1 platform. Release 4 improvements will include new models of the anisotropy of SW and LW radiation using the CERES RAP scanner as well as additional vertical levels of radiative fluxes within the atmosphere. The delay in deriving the new angular models is caused by the need for approximately two years of global observations to obtain sufficient statistical sampling for a complete range of surface and cloud conditions. Note that Release 4 will require a reprocessing of the earlier Release 2 and 3 data to provide a time-consistent climate data set for the CERES observations.

Further detailed descriptions of the CERES data products can be found in the EOS Reference Handbook and in the EOS Data Products Catalog. Both documents can be found at http://eospso.gsfc.nasa.gov. The following sections give a brief summary of the algorithms used in each of the subsystems shown in Fig. 2.

B. Subsystem 1: Instrument Geolocate and Calibrate Earth Radiances (Level 1b Data Product)

The instrument subsystem converts the raw, level 0 CERES digital count data into geolocated- and calibrated-filtered radi-
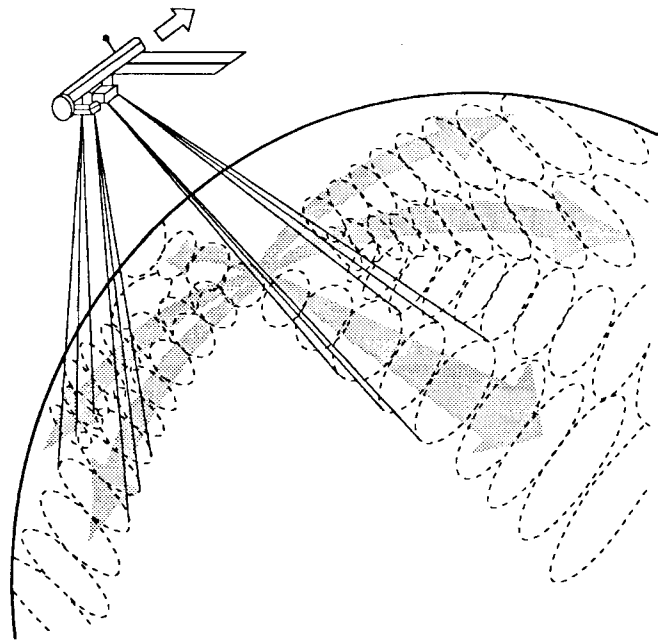

Fig. 3. Scan pattern of two CERES scanners on EOS-AM1 and EOS-PM1 spacecraft. One scanner is cross track, the other scanner rotates in azimuth angle as it scans in elevation, thereby sampling the entire hemisphere of radiation.

ances for three spectral channels: total channel (solar reflected and thermal emitted radiation from 0.3–200 μm), SW channel (solar reflected radiation from 0.3–5 μm), and LW window channel (thermal emitted radiation from 8–12 μm) [30]. Details of the conversion, including ground and onboard calibration, can be found in ATBD subsystem 1. The CERES scanners are based on the successful ERBE design, with the following modifications to improve the data.

1) Improved ground and onboard calibration by a factor of two. The accuracy goal is 1% for SW and 0.5% for LW.
2) Angular FOV reduced by a factor of two to about 20 km at nadir for the EOS-AM1 orbit altitude of 700 km. This change is made to increase the frequency of clear sky and single-layer cloud observations as well as to allow better angular resolution in the CERES-derived angular distribution models (ADM's), especially for large viewing zenith angles.
3) Improved electronics to reduce the magnitude of the ERBE offsets.
4) Improved spectral flatness in the broadband SW channel.
5) Replacement of the ERBE LW channel (nonflat spectral response) with an 8–12-μm spectral response window.

The CERES instruments are designed so that they can easily operate in pairs, as shown in Fig. 3. In this operation, one of the instruments operates in a fixed azimuth cross-track scan (CTS), which optimizes spatial sampling over the globe. The second instrument (RAP scanner) rotates its azimuth plane scan as it scans in elevation angle, thereby providing angular sampling of the entire hemisphere of radiation. The RAP scanner, when combined with cloud imager classification of cloud and surface types, will be used to provide improvements over the ERBE ADM's (ATBD subsystem 4.5). Each CERES

instrument is identical, so either instrument can operate in either the CTS or RAP scan mode. An initial set of six CERES instruments is being built, including deployment on the following

1) TRMM (1 scanner), 35° inclined precessing orbit, launched November 1997;
2) EOS-AM1 (2 scanners), 10:30 a.m. sun-synchronous orbit, launch June 1998;
3) EOS-PM1 (2 scanners), 1:30 p.m. sun-synchronous orbit, launch January 2000;
4) TRMM follow on, 57° precessing orbit 2002 (not yet confirmed).

C. Subsystem 2: ERBE-Like Inversion to Instantaneous TOA Fluxes (Level 2 ERBE-Like Data Product)

The ERBE-like Inversion Subsystem converts filtered CERES radiance measurements to instantaneous radiative flux estimates at the TOA for each CERES FOV. These ERBE-like TOA fluxes then provide the most consistent data product with historical ERBE measurements. The basis for this subsystem is the ERBE Data Management System, which produced TOA fluxes from the ERBE scanning radiometers onboard the Earth Radiation Budget Satellite (ERBS) and NOAA-9 and 10 satellites over a five-year period from November 1984 to February 1990 [1], [2]. The ERBE Inversion Subsystem [45] is a mature set of algorithms that has been well documented and tested. The strategy for the CERES ERBE-like products is to process the data through the same algorithms as those used by ERBE with only minimal changes, such as those necessary to adapt to the CERES instrument characteristics. These data products are also independent of almost all auxiliary data, such as ISCCP, VIRS, MODIS, four–dimensional (4-D) assimilation fields, etc.

D. Subsystem 3: ERBE-Like Averaging to Monthly TOA (Level 3 ERBE-Like Data Product)

This subsystem temporally interpolates the instantaneous CERES flux estimates to compute ERBE-like averages of TOA radiative parameters. CERES observations of SW and LW flux are time averaged using a data interpolation method similar to that employed by the ERBE Data Management System. The averaging process accounts for the solar zenith angle dependence of albedo during daylight hours as well as the systematic diurnal cycles of LW radiation over land surfaces [5]. The averaging algorithms produce daily, monthly-hourly, and monthly means of TOA SW and LW flux on regional, zonal, and global spatial scales. Separate calculations are performed for clear sky and total sky fluxes.

E. Subsystem 4: Overview of Cloud Retrieval and Radiative Flux Inversion (Level 2 Surface and Atmosphere Data Product)

One of the major advances of the CERES radiation budget analysis over ERBE is the ability to use time- and space-matched high-spectral and spatial resolution cloud imager data to determine cloud and surface properties within the relatively large CERES FOV (20-km diameter for EOS-AM1 and EOS-PM1, 10-km diameter for TRMM). For the first launch of the CERES broadband radiometer on TRMM in 1997, CERES uses the VIRS cloud imager as input. For the next launches on EOS-AM1 (1998) and EOS-PM1 (2000), CERES will use the MODIS cloud imager data as input. This subsystem matches imager-derived cloud properties with each CERES FOV and then uses either ERBE ADM's (Releases 1–3) or improved CERES ADM's (Release 4) to derive TOA flux estimates for each CERES FOV. Until new CERES ADM's are available three years after launch, the primary advance over the ERBE TOA flux method will be to greatly increase the accuracy of the clear sky fluxes. The limitations of ERBE clear sky determination as a result of the 40-km spatial resolution and the lack of collocated imager data cause the largest uncertainty in current estimates of cloud radiative forcing. In Release 4, using new ADM's, both rms and bias TOA flux errors for all scenes are expected to be a factor of three–four smaller than those for the ERBE-like analysis.

In addition to improved TOA fluxes, this subsystem also provides the CERES FOV matched cloud properties used by subsystem 5 to calculate radiative fluxes at the surface and within the atmosphere that are consistent with the TOA fluxes for each CERES FOV. Finally, this subsystem also provides estimates of surface fluxes using direct TOA-to-surface parameterizations. Because of its complexity, this subsystem has been further decomposed into six additional subsystems.

1) Imager Clear Sky Determination and Cloud Detection: This subsystem is an extension of the ISCCP time-history approach with several key improvements, including the use of the following:

a) multispectral clear/cloud tests (see [21]);
b) improved spatial and spectral resolution clear sky background maps;
c) improved calibration for VIRS and especially MODIS; and
d) improved navigation (approximately 3 km for TRMM and <1 km for EOS-AM1).

2) Imager Cloud Height Determination: For ISCCP, this step is part of the cloud property determination. CERES separates this step and allows the use of the following three independent techniques to search for well-defined cloud layers:

a) comparisons of multispectral histogram analyses to theoretical calculations [36];
b) spatial coherence [14]; and
c) infrared sounder radiance ratioing (15-μm band channels) [4], [34] (available for MODIS only).

While the analysis of multilevel clouds is at an early development stage, it is considered a critical area and will be examined even in Release 2 of the CERES algorithms. The need for identification of multilayer clouds arises from the sensitivity of surface downward LW flux to low-level clouds and cloud overlap assumptions. Release 2 will only attempt to classify which imager pixels contain overlapping clouds. Later releases will examine the potential to derive multiple cloud layers. There are two promising techniques for deriving multiple cloud layers from satellite: a combination of infrared sounder data for high optically thin cloud and imager data for
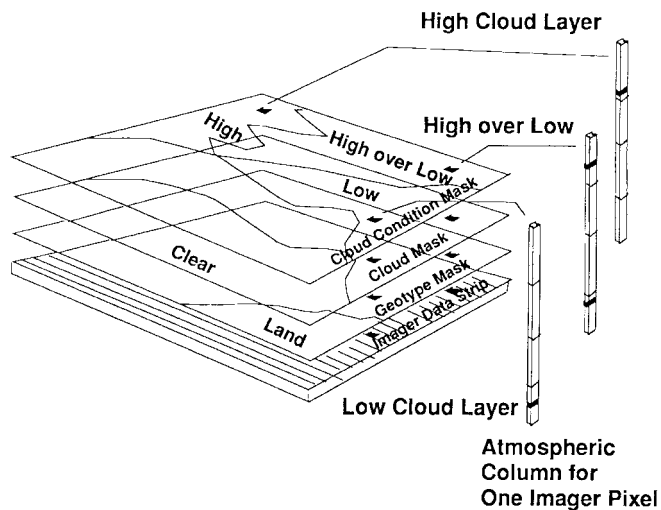
Fig. 4.   Illustration of the CERES cloud algorithm using cloud imager data from VIRS and MODIS. Imager data are overlaid by a geographic scene map, cloud mask, and cloud overlap condition mask. For each imager FOV, cloud properties are determined for one cloud layer (Release 2) or up to two cloud layers (Releases 3 and 4).
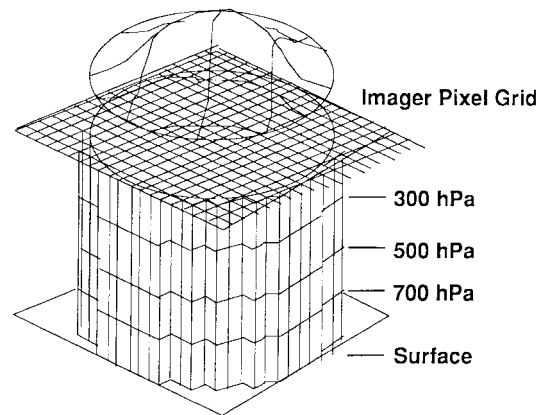

Fig. 5.   Illustration of the Gaussian-like point spread function for a single CERES FOV, overlaid over a grid of cloud imager pixel data. The four vertical layers represent the CERES cloud height categories, which are separated at 700, 500, and 300 hPa. Cloud properties are weighted by the point spread function to match cloud and radiative flux data.

an underlying low thick cloud, as shown in Baum *et al.* [4], and a combination of imager data for high thick ice cloud and passive microwave for an underlying low thick water cloud over the ocean, as shown in Lin *et al.* [33].

3) Cloud Optical Property Retrieval: For ISCCP, this step involves the determination of a cloud optical depth using visible channel reflectance. An infrared emittance is derived using this visible optical depth along with an assumption of cloud microphysics (10-μm water spheres for warm clouds and ice polycrystals for cold clouds). Finally, during daytime, ISCCP uses the cloud infrared emittance estimate to correct the cloud radiating temperature for nonblack clouds. The CERES analysis extends these properties to include cloud particle size and phase estimation by using additional spectral channels at 1.6 and 3.7 μm (TRMM, MODIS) or 1.6 and 2.1 μm (MODIS) during the day [28], [35] and 3.7 and 8.5 μm (TRMM, MODIS) at night. In addition, the use of infrared sounder channels in subsystem 4.2 allows correction for the presence of nonblack cirrus cloud for both daytime and nighttime conditions [4], [34]. The CERES cloud property analysis scheme illustrated in Fig. 4 shows a schematic drawing showing the cloud imager pixel data overlaid with a geographic mask of surface type and elevation, the cloud mask from subsystem 4.1, the cloud height and overlap conditions specified in subsystem 4.2, and the column of cloud properties for each imager pixel in the analysis region.

4) Convolution of Imager Cloud Properties with CERES Footprint Point Spread Function: For each CERES FOV, the CERES point spread function is roughly Gaussian in shape (top of Fig. 5) and is used to weight the individual cloud imager footprint data to provide cloud properties matched in space and time to the CERES broadband radiance measurements [37]. The 20-km CERES FOV size at nadir is the distance between the 50% response points in the response function. The point spread response function is a spatial domain analog of a spectral response function for a narrowband cloud imager spectral channel. Because cloud

radiative properties are nonlinearly related to cloud optical depth, a frequency distribution of cloud optical depth is kept for each cloud height category in a CERES FOV.

5) CERES Inversion to Instantaneous TOA Fluxes: The cloud properties determined for each CERES FOV are used to select an ADM class to convert measured broadband radiance into an estimate of TOA radiative flux. In Releases 1–3, the ERBE ADM classes will be used. After several years of CERES RAP scanner data have been obtained, new ADM's will be developed as a function of cloud amount, cloud height, cloud optical depth, and cloud particle phase and size. An important characteristic of these empirical ADM's is that they do not rely on plane-parallel radiative transfer theory and can, therefore, include the effect of three-dimensional (3-D) cloud structure. For clear sky conditions, a range of clear sky land ADM classes will be made based on the 17 International Geosphere–Biosphere Program (IGBP) land cover classes. Several ocean ADM's will be made based on surface wind speed.

6) Empirical Estimates of Surface Shortwave and Longwave Radiative Fluxes Based on CERES TOA Flux Measurements: This subsystem uses parameterizations to directly relate the CERES TOA fluxes to surface fluxes. There are three primary advantages to using parameterizations, as follows:

1) can be directly verified against surface measurements;
2) maximizes the use of the CERES calibrated TOA fluxes; and
3) computationally simple and efficient.

There are two primary disadvantages to this approach, as follows:

1) difficult to obtain sufficient surface data to verify direct parameterizations under all cloud, surface, and atmosphere conditions; and
2) may not be able to estimate all individual upward and downward surface fluxes with sufficient accuracy, especially downward LW flux at the surface under cloudy sky conditions.

For Release 2, we have identified parameterizations to derive surface net SW radiation [8], [32], clear sky downward LW flux [27], and total sky downward LW flux [19], [20]. Recent

studies [9], [39] have questioned the applicability of the [32] surface SW flux algorithm, but this algorithm will be used in Release 2, pending the results of further validation.

The combined importance and difficulty of deriving surface radiative fluxes has led CERES to a twofold approach. The results using the parameterizations given in subsystem 4.6 are saved in the CERES Surface Product. A separate approach using the imager cloud properties, radiative transfer models, and TOA fluxes is summarized in subsystem 5.0, and these surface fluxes are saved in the CERES Atmosphere Products. Both of the approaches in subsystems 5.0 and 4.6 use radiative modeling to varying degrees. The difference is that the radiative models in the Surface Product are used to derive the form of a simplified parameterization between satellite observations and surface radiative fluxes. The satellite observations are primarily CERES TOA fluxes, but they include selected auxiliary observations, such as column water vapor amount. These simplified surface flux parameterizations are then tested against surface radiative flux observations. If necessary, the coefficients of the parameterizations are adjusted to obtain the optimal consistency with the surface observations.

Ultimately, the goal is to improve the radiative modeling and physical understanding to the point where they are more accurate than the simple parameterizations used in the Surface Product. In the near-term, validation against surface observations of both methods in subsystems 4.6 and 5.0 will be used to determine the most accurate approach. If the simplified surface flux parameterizations prove more accurate, the surface fluxes derived in subsystem 4.6 will also be used as a constraint on the calculations of in-atmosphere fluxes derived in subsystem 5.0. This would be a weaker constraint than TOA fluxes, given the larger expected errors for the surface flux estimates.

F. Subsystem 5: Compute Surface and Atmospheric Fluxes (Level 2 ATMOSPHERE Data Product)

This subsystem is commonly known as Surface and Atmospheric Radiation Budget (SARB) and uses an alternate approach to obtain surface radiative fluxes as well as obtaining estimates of radiative fluxes at predefined levels within the atmosphere. All SARB fluxes include SW and LW fluxes for both up and down components of the flux at all defined output levels from the surface to the TOA. For Release 2 (shown in Fig. 1), output levels are the surface, 500 hPa, 70 hPa, and TOA. The major steps in the SARB algorithm for each CERES FOV include the following:

1) input surface data (albedo, emissivity);
2) input meteorological data (T, q, O_3, aerosol);
3) input imager cloud properties matched to CERES FOV's;
4) use radiative model to calculate radiative fluxes from observed properties;
5) adjust surface and atmospheric parameters (e.g., cloud or precipitable water) to get consistency with CERES observed TOA SW and LW fluxes; constrain parameters to achieve consistency with subsystem 4.6 surface flux estimates if validation studies show these surface fluxes

to be more accurate than radiative model computations of surface fluxes; and
6) save final flux calculations, initial TOA discrepancies, and surface/atmosphere property adjustments along with original surface and cloud properties.

While global TOA fluxes have been estimated from satellites for more than 20 years, credible, global estimates for surface and in-atmosphere fluxes have only been produced globally in the last few years [11], [15], [20], [32], [38], [48], [57]. Key outstanding issues for SARB calculations include the following:

1) cloud layer overlap, which primarily affects the surface and atmosphere LW fluxes [12];
2) effect of cloud inhomogeneity [3], [6];
3) 3-D cloud effects [24], [44];
4) potential enhanced cloud absorption [9], [39], [46]; and
5) land surface bidirectional reflection functions, emissivity, and surface skin temperature.

For Release 2, SARB will use plane-parallel radiative model calculations and will treat cloud inhomogeneity by performing separate radiative computations for up to two nonoverlapped cloud layers in each CERES FOV. The average CERES FOV optical depth for each cloud layer is defined by averaging the logarithm of imager pixel optical depth values, each weighted by the CERES point spread function. The logarithmic averaging of optical depth uses the assumption that albedo varies more linearly with the logarithm of optical depth [42]. This reduces the uniform plane parallel bias noted by Barker *et al.* [3] and Cahalan *et al.* [6].

For Release 2, adjustment of the calculated fluxes to consistency with the CERES instantaneous TOA fluxes can be thought of as providing an "equivalent plane-parallel" cloud. For example, consider a fair weather cumulus field over Brazil viewed from the CERES and MODIS instruments. Because the CERES ADM's are developed as empirical models that are a function of cloud amount, cloud height, and cloud optical depth, the CERES radiative flux estimates can implicitly include 3-D cloud effects for broken boundary layer cumulus and, in principle, can produce unbiased TOA flux estimates. Note that this would not be true if CERES had inverted radiance to flux using plane-parallel theoretical models. The cloud optical depth derived from MODIS data, however, has been derived using a plane-parallel retrieval. If this imager cloud optical depth is in error because of 3-D cloud effects, the calculated SARB TOA SW flux will be in error and the cloud optical depth will be adjusted to compensate, thereby achieving a plane-parallel cloud optical depth that gives the same reflected flux as the 3-D cloud. In an analogous fashion for the LW fluxes, cloud amount might require adjustment to remove 3-D cloud artifacts. In all cases, cloud property changes are applied consistently to calculations of both SW and LW fluxes.

Tests against measured surface fluxes will be required to verify if these adjustments to the model TOA fluxes and cloud properties can consistently and accurately reproduce the surface fluxes. These comparisons have begun using the ARM Oklahoma Intensive Observing Periods (IOP's) in a

joint CERES/ARM/GEWEX effort called CAGEX [10]. The CAGEX results and data sets can be accessed on the web using http://snowdog.larc.nasa.gov:8081/cagex.html. The data products from the SARB calculations will include both the magnitude of the required surface and cloud property adjustments as well as the initial and final differences between calculated and TOA measured fluxes. An example calculation of LW fluxes and LW atmospheric heating rate both before and after adjustment to match TOA observations using the ERBE data is illustrated in Fig. 6 for a clear sky ocean case. FL refers to the radiative transfer model of Fu and Liou [17], [18] and is the baseline radiative transfer model used for CERES SW and LW radiative calculations. HCW is a comparison radiative model calculation using Harshvardhan *et al.* [16] and Wang *et al.* [51] for LW fluxes and Chou [13] for SW fluxes. In the clear sky ocean case shown in Fig. 6, differences in the radiative models are larger than the adjustments required to match the ERBE TOA fluxes. For Releases 1 and 2, this approach is tested using AVHRR and HIRS data to derive cloud properties and ERBE TOA flux data to constrain the calculations at the TOA.

G. Subsystem 6: Grid Single Satellite Fluxes and Clouds and Compute Spatial Averages (Level 3 ATMOSPHERE Data Product)

The next step in the processing of the CERES Atmosphere Data Products is to grid the instantaneous CERES FOV data output from subsystem 5.0 into the EOS standard 1° equal angle grid boxes. Note that all CERES level 2 (FOV) data products are stored in 1-h orbit segments along the satellite ground track. This method was chosen to simplify later subsetting of the data, to reduce data volumes, and to simplify sorting for later time interpolation of multiple satellite data products. The 1° equal angle grid was chosen by EOS to simplify comparisons to global land, ocean, and atmosphere models. At high latitudes, where the distance between longitudinal steps becomes smaller, CERES will increase the longitude steps by factors of two to maintain consistent accuracy in the gridding process. Cloud properties and TOA fluxes from subsystem 4 and the additional surface and atmospheric radiative fluxes added in subsystem 5 are weighted by their respective area coverage in each grid box.

While spatial averaging of surface, atmosphere, and TOA radiative fluxes is relatively straightforward, spatial averaging of cloud properties is not so straightforward. The issue is most obvious when we consider the following thought experiment. We compare monthly average 1° gridded LW TOA fluxes in the tropical Pacific Ocean for June of two years, one that was during an ENSO (El Niño/Southern Oscillation) event and one that was not. We find a large change in TOA LW flux and want to know what change in cloud properties caused the change: cloud amount, cloud height, or cloud optical depth? Because cloud properties are nonlinearly related to radiative fluxes, and if we have simply averaged over all of those nonlinear relationships, we cannot guarantee that the question has an unambiguous answer. For example, consider that for TOA LW flux, changes in cloud amount or optical depth of a high
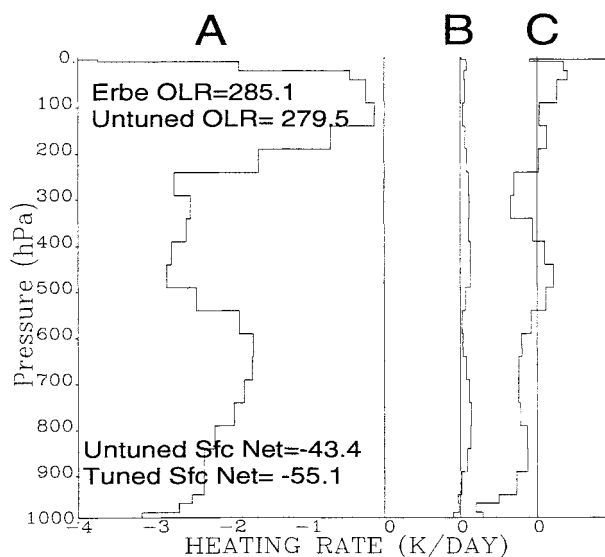

Fig. 6. Test analysis of a clear-sky ERBE FOV over the ocean using NMC temperature and water vapor. Initial calculation of TOA LW flux is in error by 5.6 Wm^{-2}, and the water vapor amount is tuned to match the TOA value. Curve A shows the tuned LW heating rate profile (degrees/day). Curve B shows the difference between tuned and untuned heating rates. Curve C shows the difference between the calculations of two different radiative transfer models.

altitude cloud have a large effect on LW flux. For low clouds, they have almost no effect. Cloud height changes of either low or high clouds will have a roughly similar effect. If we had instead considered a change in surface downward LW flux, the low clouds would dominate and the high clouds would have little effect. These are exactly the type of changes we need to examine and understand to address issues of cloud/climate feedback. If we carry this analogy further, we can see that it is important to consider the impact of cloud changes on at least five basic parameters, as follows:

1) LW upward TOA flux;
2) LW downward surface flux;
3) SW upward TOA or downward surface flux (expected to be roughly linearly related);
4) liquid water volume; and
5) ice water volume.

The first three of these parameters are critical to cloud radiative forcing issues, and the last two are critical to cloud dynamical modeling. We could also add in-atmosphere LW and SW net fluxes, but the five above are a good start. While the CERES team has not yet resolved the optimal way to average cloud properties, it has included in the data structures the capability to experiment using the early postlaunch data with various formulations. Global circulation model simulations will also be very useful in understanding the optimal methods to composite cloud properties.

H. Subsystem 7: Time Interpolation and Synoptic Flux Computation for Single and Multiple Satellites (Level 3 ATMOSPHERE Data Product)

Starting in January 1998, CERES will have one precessing satellite (TRMM) sampling each location on the earth twice per day from roughly 40° S to 40° N. In June 1998, the

EOS-AM1 platform with a 10:30 a.m. sun-synchronous orbit will increase diurnal sampling to four times per day for most of the earth. In 2000, the EOS-PM1 satellite with a 1:30 p.m. sun-synchronous orbit will be launched. If TRMM is still functioning, or when a TRMM follow-on is launched, CERES will then have its design goal of six samples per day. Simulation studies using hourly GOES data indicate that the ERBE time-space averaging algorithm gives regional monthly mean time sampling errors (1σ), which are approximately as follows:

1) 9 W-m^{-2} for TRMM alone;
2) 4 W-m^{-2} for TRMM plus EOS-AM1; and
3) 2 W-m^{-2} for TRMM plus EOS-AM1 plus EOS-PM1.

Since satellites can fail prematurely, it is useful to provide a strategy to reduce time sampling errors, especially for the single satellite case.

The CERES strategy is to incorporate three-hourly GEO radiance data to provide a correction for diurnal cycles that are insufficiently sampled by the CERES samples from EOS-AM1, EOS-PM1, and TRMM. The key to this strategy is to use the GEO data to supplement the shape of the diurnal cycle, but then use the CERES observations as the absolute reference to anchor the more poorly-calibrated GEO data (Fig. 7). One advantage of this method is that it produces three-hourly synoptic radiation fields, both for use in global model testing and for improved examination of diurnal cycles of clouds and radiation. The output of subsystem 7 is a 1° gridded estimate of cloud properties and surface, atmosphere, and TOA fluxes at each three-hourly synoptic time. These estimates are also used later in subsystem 8 to aid in the production of monthly average cloud and radiation data.

The process for synoptic processing involves the following steps.

1) For each 1° region, temporally sort the CERES TRMM, EOS-AM1, and EOS-PM1 gridded cloud and radiation data produced by subsystem 6.
2) For each 1° region, temporally sort the three-hourly near-synoptic GEO data.
3) Interpolate cloud properties from the CERES times of observation to the synoptic times.
4) Use the cloud properties to select an ADM scene class, convert the narrowband GOES radiance to broadband (using regional correlations to CERES broadband observations), and then convert the broadband radiance to broadband TOA flux (using the CERES broadband ADM's).
5) Use the diurnal shape of the radiation fields derived from GEO data, but adjust this shape to match the CERES times of observations to account for calibration errors in the GEO data.
6) Use the time-interpolated cloud properties to calculate radiative flux profiles, as in subsystem 5, using the synoptic TOA flux estimates as a constraint.

The system described above could also use the ISCCP GEO cloud properties. The disadvantage of this approach is that it incorporates cloud properties that are systematically different and less accurate than those from the cloud imagers flying
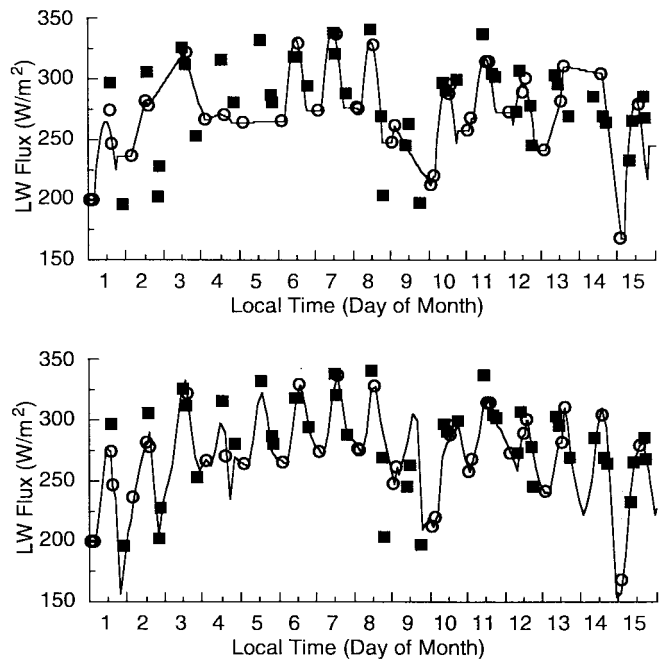

Fig. 7. Time series of ERBE ERBS (solid squares) and NOAA-9 (open circles) LW flux observations and interpolated values from July 1985 over New Mexico. Top curve shows the ERBE time-interpolated values; bottom curve shows the GEO data-enhanced interpolation.

with CERES. The ISCCP cloud properties are limited by GEO spatial resolution, spectral channels, and calibration accuracy. In this sense, it would be necessary to "calibrate" the ISCCP cloud properties against the TRMM and EOS cloud properties. We are currently performing sensitivity studies on the utility of the ISCCP cloud properties for this purpose.

I. Subsystem 8: Monthly Regional, Zonal, and Global Radiation Fluxes and Cloud Properties (ATMOSPHERE Data Product)

This subsystem uses the CERES instantaneous radiative flux and cloud data (TRMM, EOS-AM1, EOS-PM1 observation times) as well as the synoptic radiative flux and cloud data (subsystem 7) and time averages to produce monthly averages at regional, zonal, and global spatial scales. Initial simulations using both one- and three-hourly data have shown that simple averaging of the three-hourly results is adequate for calculating monthly average LW fluxes. SW flux averaging, however, is more problematic. The magnitude of the solar flux diurnal cycle is ten to 100 times larger than that for the LW flux.

For SW flux time averaging, a key issue is to avoid biases caused by the systematic increase of albedo with solar zenith angle between times of observation as well as between sunset and sunrise and the first daytime observation. The CERES SW flux time averaging procedure [22] starts from the three-hourly synoptic data, and then time interpolates to a finer resolution time grid using methods analogous to ERBE [5] for other hours of the day with significant solar illumination. Validation of these time interpolation techniques for SW radiation at the surface are being carried out using surface measurements of solar insolation, such as those provided by the ARM or BSRN sites [22].

J. Subsystem 9: Grid TOA and Surface Fluxes for Instantaneous Surface Product (Level 3 SURFACE Data Product)

This subsystem is essentially the same process as in subsystem 6. The major difference is that instead of gridding data to be used in the Atmosphere Data Products (subsystems 5–8), this subsystem spatially grids the data to be used in the Surface Data Products (subsystems 9 and 10). The spatial grid is the same: 1° equal angle. See the data flow diagram (Fig. 2) and the discussion in Section III-E6 and III-F for a summary of the difference between the Atmosphere and Surface Data Products.

K. Subsystem 10: Monthly Regional TOA and Surface Radiation Budget (SURFACE Data Product)

The time averaging for the Surface Data Product is produced by two methods. The first method is the same as the ERBE method that produces the ERBE-like product in subsystem 3 with the following exceptions:

1) improved CERES ADM's for the scene-dependent solar zenith angle dependence of albedo;
2) improved CERES ADM's for the scene-dependent solar zenith angle dependence of albedo;
3) improved cloud imager scene identification (subsystem 4) and improved CERES ADM's to provide more accurate instantaneous TOA fluxes.

Simulation studies indicate that for this method the monthly averaged fluxes will be a factor of two–three more accurate than the ERBE-like fluxes.

The second method incorporates GEO radiances similar to the process outlined for synoptic products in subsystem 7. We include this method to minimize problems during the initial flight with TRMM when we have only one spacecraft with two samples per day. As the number of satellites increases to three, the GEO data will have little impact on the results. Because one of the major rationales for the Surface Data Products is to keep surface flux estimates as closely tied to the CERES direct observations as possible, this subsystem will not calculate in-atmosphere fluxes and will derive its estimates of the surface fluxes using the parameterizations discussed in subsystem 4.6. This level 3 Surface Data Product will also have a much smaller data volume than the Atmosphere Data Product.

L. Subsystem 11: Grid GEO Narrowband Radiances

CERES will use three-hourly GEO radiance data to assist diurnal modeling of TOA fluxes and minimize temporal interpolation errors in CERES monthly mean TOA flux products. This subsystem is essentially the same process as in subsystem 6. The major difference is that the process is performed on GEO radiances instead of CERES TOA fluxes. The current input data to the CERES algorithms are one month of three-hourly ISCCP B1 GEO data, which contain visible and infrared narrowband radiances from different satellites. At the present time, GEO data are available for four satellites: METEOSAT, GOES-East, GOES-West, and GMS. Negotiations are under-way to use either INSAT or the Chinese FY-2 satellite as the fifth GEO satellite for ISCCP. The spatial resolution of the GEO data sets is approximately 4–10 km. These data are gridded and spatially averaged into CERES 1° equal angle grid boxes using functions described in subsystem 6. The outputs consist of statistics (e.g., mean) of the visible and infrared narrowband radiances for each of the CERES 1° grid boxes and each of the three-hourly synoptic times. This data product represents a major input source for both subsystems 7 and 10.

M. Subsystem 12: Regrid Humidity and Temperature Fields

This subsystem interpolates temperature, water vapor, ozone, aerosols, and passive microwave column water vapor obtained from diverse sources to the spatial and temporal resolution required by various CERES subsystems. Most of the inputs come from EOS Data Assimilation Office (DAO) or NOAA NCEP 4-D analysis products, although the subsystem accepts input from many different sources on many different grids. The outputs consist of the same meteorological fields as the inputs, but at a uniform spatial and temporal resolution necessary to meet the requirements of the other CERES processing subsystems. Interpolation methods vary, depending on the nature of the field. For Release 2, CERES is planning to use the DAO analysis products. One of the key issues for use of analysis products in a climate data set is the "freezing" of the analysis product algorithms during the climate record. DAO has agreed to provide a consistent analysis method for CERES.

IV. RELATIONSHIPS TO OTHER EOS INSTRUMENTS AND NON-EOS FIELD EXPERIMENTS: ALGORITHM VALIDATION AND INTERDISCIPLINARY STUDIES

While the direct ties to VIRS on TRMM and MODIS on EOS have been obvious throughout this overview, there are indirect ties between the CERES data products and many of the EOS instruments. Furthermore, there is an opportunity to substantially increase the ability to detect cloud overlap by using the passive microwave retrievals of cloud liquid water path from the TRMM Microwave Imager (TMI) as well as the Advanced Microwave Scanning Radiometer (AMSR) instrument on EOS-PM1 (2001). METOP (2001) is the morning sun-synchronous European meteorological satellite that may provide passive microwave data in the same orbit as the EOS-AM1 platform. This constellation of instruments would allow a three-satellite system with CERES/cloud imager/passive microwave instruments on each spacecraft. This suite provides both adequate diurnal coverage as well as a greatly increased ability to detect the presence of multilayer clouds, even beneath a thick cirrus shield. Passive microwave liquid water path retrievals will be tested using TRMM data for multilayer clouds over the ocean and may be included for Release 4.

The Multi-angle Imaging SpectroRadiometer (MISR) and Advanced Spaceborne Thermal Emission and Reflection Radiometer (ASTER) onboard the EOS-AM1 platform will provide key validation data for the CERES experiment. MISR can view 300-km wide targets on the earth nearly simultaneously (within 10 min) from nine viewing zenith angles using nine separate charge-coupled device (CCD) array cameras. This

capability provides independent verification of CERES SW bidirectional reflectance models as well as stereo cloud height observations. For radiative fluxes, MISR has better angular sampling than CERES, but at the price of poorer time and spectral information (narrowband instead of broadband). The Polarization of Directionality of Earth's Reflectances (POLDER) instrument launched on the Advanced Earth Observing System (ADEOS-1) platform in 1996 and on ADEOS-2 in 2000 will also allow tests of CERES anisotropic models using narrowband models. ASTER on the EOS-AM1 platform will provide Landsat-like very high spatial resolution data to test the effect of MODIS and VIRS coarser resolution data (i.e., beam filling problems) on the derivation of cloud properties.

In September 1994, the Lidar In-Space Technology Experiment (LITE) provided the first high-quality global lidar observations of cloud height from space. These data will be a key source for determining the spatial scale of cloud height variations around the globe. Unfortunately, the limited duty cycle of lidar data collection during the two-week space shuttle mission resulted in only a few coincidences with GOES, SSM/I, or NOAA polar orbiting spacecraft. Nevertheless, the limited data available showed that unlike aircraft- or surface-based lidar, the space-based lidar could penetrate to the top of boundary layer cloud or to the surface of the earth at least 80% of the time [59]; due to additional forward scattered photons that remain within the relatively large space-based lidar field of view of 300 m.

Given the relative importance of multilayered cloud to calculations of LW surface and atmospheric radiative fluxes, clearly a space-based cloud lidar and/or radar mission is essential in the future. Recent studies in support of NASA's new Earth System Science Pathfinder (ESSP) program indicate that the ideal combination to resolve all multilayered cloud is a lidar for optically thin and physically thin cloud layers, combined with a cloud radar (3- or 8-mm wavelength) for optically and physically thick cloud layers. Space-based cloud lidar can resolve thin clouds to 50-m vertical resolution, while cloud radar has a vertical resolution of about 500 m. At the same time, a cloud radar will be able to observe optically thick layers (visible optical thickness greater than about ten), which will attenuate the lidar signal. A combined lidar/radar mission that synchronized its orbit with the EOS-AM1 or EOS-PM1 would be ideal for global validation of CERES and EOS cloud properties, including the difficult polar cloud cases. Spaceborne cloud radar has been endorsed as a high priority mission by the [Global Energy and Water Cycle Experiment (GEWEX)] of the World Climate Research Program. The Geoscience Laser Altimetry System (GLAS), scheduled for launch in 2002, is planned to include cloud lidar capability, but the orbit optimization required for its primary mission (i.e., measuring ice sheet volume) is not optimal for validation of EOS cloud properties. As currently planned, GLAS will obtain about 1% of its data (approximately 10% of one month each year) nearly simultaneous (±6 min) with EOS-AM1 or EOS-PM1, depending on the final selected orbit altitude.

Established surface sites (e.g., ARM, BSRN, and SURFMAP) will provide one of the most critical sources of validation for CERES surface radiative fluxes and cloud properties. The ARM sites in Oklahoma, the tropical western Pacific Ocean, and the north slope of Alaska will provide the most critical long-term time series of validation data. These sites will include measurements of SW and LW surface fluxes, cloud base height from lidar, multiple cloud layers from cloud radar, passive microwave-derived liquid water path, and newly developing estimates of the vertical profiles of cloud microphysics in both water and ice cloud layers. The newly developing ARM vertical profiles of cloud microphysics and cloud boundaries will be critical for validation of satellite-derived cloud properties. Because thousands of cases are needed to provide stable error statistics as a function of cloud type and satellite viewing condition, CERES is proposing a bootstrapped approach to satellite cloud property validation. First, *in situ* aircraft microphysical data are used to validate the ARM site vertical cloud profiling capabilities based on combining cloud lidar, radar, and passive radiometer data. Then in turn, the ARM time series of cloud properties is used to validate all satellite overpasses of the ARM sites over a period of several years. The resulting large number of validation cases are used to gather robust statistics on the accuracy of cloud remote sensing as a function of cloud type and satellite viewing condition (e.g., day, night, nadir view, and large viewing zenith angles). For surface fluxes, the BSRN sites will provide additional sites for carefully calibrated and maintained SW and LW surface fluxes. The major limitation of the ARM sites will be the lack of observations in other important climatic regimes, such as desert, midlatitude ocean, tropical land, subtropical ocean, and heavily vegetated midlatitude land. The major limitation of the BSRN sites is the lack of quantitative cloud data. To mitigate some of this difficulty, CERES will be placing micropulse lidar systems for cloud base measurements at BSRN sites in Bermuda, Saudi Arabia, and at a tropical land site.

Finally, field experiment campaigns will be necessary to extend the climatological regimes sampled by the ARM and BSRN sites. These campaigns will allow coordination of surface and *in situ* aircraft measurements of cloud properties and radiative fluxes during overpasses of the EOS spacecraft. CERES science team members are active participants on the FIRE, ARM, and GEWEX experiment teams. CERES will rely on these national and international programs to provide critical validation data. It is expected that the accuracy of CERES validation efforts will systematically improve as additional surface/satellite and field experiment/satellite coincidences are obtained. A large number of such coincidences will be required to validate the wide range of cloud and climate conditions within the global climate system. Validation plan drafts have been prepared for each of the CERES data products and were reviewed in Spring 1997. The plans are currently available on the same World Wide Web site as the CERES ATBD's.

would like to thank K. Costulis for extensive assistance in preparation of the CERES algorithm documentation, both in the present paper and in the entire set of CERES Algorithm Theoretical Basis Documents available on the World Wide Web. Comments by two reviewers also contributed substantially to the clarity of the paper.

REFERENCES

[1] B. R. Barkstrom, "The earth radiation budget experiment (ERBE)," *Bull. Amer. Meteorol. Soc.,* vol. 65, pp. 1170–1185, 1984.

[2] B. R. Barkstrom and G. L. Smith, "The earth radiation budget experiment: Science and implementation," *Rev. Geophys.,* vol. 24, pp. 379–390, 1986.

[3] H. W. Barker, B. A. Wielicki, and L. Parker, "A parameterization for computing grid-averaged solar fluxes for inhomogeneous marine boundary layer clouds. Part II: Validation using satellite data," *J. Atmos. Sci.,* vol. 53, pp. 2304–2316, 1996.

[4] B. A. Baum, R. F. Arduini, B. A. Wielicki, P. Minnis, and S.-C. Tsay, "Multilevel cloud retrieval using multispectral HIRS and AVHRR data: Nighttime oceanic analysis," *J. Geophys., Res.,* vol. 99, no. D3, pp. 5499–5514, 1994.

[5] D. R. Brooks, E. F. Harrison, P. Minnis, J. T. Suttles, and R. S. Kandel, "Development of algorithms for understanding the temporal and spatial variability of the earth's radiation balance," *Rev. Geophys.,* vol. 24, pp. 422–438, 1986.

[6] R. F. Cahalan, W. Ridgway, W. J. Wiscombe, S. Gollmer, and Harshvardhan "Independent pixel and Monte Carlo estimates of stratocumulus albedo," *J. Atmos. Sci.,* vol. 51, no. 24, pp. 3776–3790, 1994.

[7] CEES Our Changing Planet, The FY 1994 U.S. Global Change Res. Program, Nat. Sci. Foundation, Washington, DC, 1994, p. 84.

[8] R. D. Cess, F. Jiang, E. G. Dutton, and J. J. Deluisi, "Determining surface solar absorption from broadband satellite measurements for clear skies—Comparison with surface measurements," *J. Clim.,* vol. 4, pp. 236–247, 1991.

[9] R. D. Cess, M. H. Zhang, P. Minnis, L. Corsetti, E. G. Dutton, B. W. Forgan, D. P. Garber, W. L. Gates, J. J. Hack, and E. F. Harrison, "Absorption of solar radiation by clouds: Observations versus models," *Science,* vol. 267, no. 5197, pp. 496–498, 1995.

[10] T. P. Charlock and T. L. Alberta, "The CERES/ARM/GEWEX experiment (CAGEX) for the retrieval of radiative fluxes with satellite data," *Bull. Amer. Met. Soc.,* vol. 77, no. 11, pp. 2673–2683, 1996.

[11] T. P. Charlock, F. G. Rose, S.-K. Yang, T. Alberta, and G. L. Smith, "An observational study of the interaction of clouds, radiation, and the general circulation," in *Proc. IRS 92: Current Problems Atmos. Rad.* Hampton, VA: Deepak, 1993, pp. 151–154.

[12] T. P. Charlock, F. Rose, T. Alberta, G. L. Smith, D. Rutan, N. Manalo-Smith, P. Minnis, and B. A. Wielicki, "Cloud profiling radar requirements: Perspective from retrievals of the surface and atmosphere radiation budget and studies of atmosphere energetics," in *Appendix B in Utility and Feasibility of a Cloud Profiling Radar,* WMO/TD 593, IGPO Pub. Series 10, p. 46, 1994.

[13] Chou, "A solar radiation model for use in climate studies," *J. Atmos. Sci.,* vol. 49, pp. 762–772, 1992.

[14] J. A. Coakley, Jr. and F. P. Bretherton, "Cloud cover from high-resolution scanner data—Detecting and allowing for partially filled fields of view," *J. Geophys. Res.,* vol. 87, pp. 4917–4932, 1982.

[15] W. L. Darnell, W. F. Staylor, S. K. Gupta, N. A. Ritchey, and A. C. Wilber, "Seasonal variation of surface radiation budget derived from international satellite cloud climatology project C1 data." *J. Geophys. Res.,* vol. 97, no. D14, pp. 15741–15760, 1992.

[16] D. R. Harshvardhan, D. A. Randall, and T. G. Corsetti, "A fast radiation parameterization for atmospheric circulation models," *J. Geophys. Res.,* vol. 92, pp. 1009–1016, 1987.

[17] Q. Fu and K.-N. Liou, "On the correlated-K distribution method for radiative transfer in nonhomogeneous atmospheres," *J. Atmos. Sci.,* vol. 49, pp. 2139–2156, 1992.

[18] ——, "Parameterization of the radiative properties of cirrus clouds," *J. Atmos. Sci.,* vol. 50, pp. 2008–2025, 1993.

[19] S. K. Gupta, "A parameterization for longwave surface radiation from sun-synchronous satellite data," *J. Clim.,* vol. 2, pp. 305–320, 1989.

[20] S. K. Gupta, W. L. Darnell, and A. C. Wilber, "A parameterization for longwave surface radiation from satellite data—Recent improvements," *J. Appl. Meteorol.,* vol. 31, no. 12, pp. 1361–1367, 1992.

[21] G. B. Gustafson *et al.,* Support of environmental requirements for cloud analysis and archive (SERCAA): Algorithm descriptions, Phillips Lab.,

Hanscom AFB, MA, Rep. PL-TR-94-2114, 1994, p. 108.

[22] M. P. Haeffelin, T. Wong, and D. F. Young, "Temporal sampling errors in atmospheric and surface fluxes," in *Preprints, 10th Conf. Appl. Clim.* Reno, NV: Amer. Meteor. Soc., 1997, pp. 80–84.

[23] J. Hansen, A. Lacis, R. Ruedy, M. Sato, and H. Wilson, "How sensitive is the world's climate," *Nat. Geogr. Res. Explor.,* vol. 9, no. 2, pp. 142–158, 1993.

[24] A. Hiedinger and S. Cox, "Radiative surface forcing of boundary layer clouds," in *8th Conf. Atmos. Rad.,* 1994, pp. 246–248.

[25] J. T. Houghton, G. J. Jenkins, and J. J. Ephraums, Eds., *Climate Change: The IPCC Scientific Assessment.* Cambridge, U.K.: Cambridge Univ. Press, 1990, IBSN: 0 521 40360 X, p. 364

[26] J. T. Houghton, L. G. Meira Filho, B. A. Callender, N. Harris, A. Kattenber, and K. Maskell, Eds., *Climate Change 1995: The Science of Climate Change.* Cambridge, U.K.: Cambridge Univ. Press, 1996, ISBN: 0-521-56433-6, p. 572.

[27] A. K. Inamdar and V. Ramanathan, "On monitoring the water vapor feedback from space: Demonstration with CERES instrument," *Tellus,* to be published.

[28] M. D. King, Y. J. Kaufman, W. P. Menzel, and D. D. Tanré, "Remote sensing of cloud, aerosol, and water vapor properties from the moderate resolution imaging spectrometer (MODIS)," *IEEE Trans. Geosci. Remote Sensing,* vol. 30, pp. 2–27, Jan. 1992.

[29] S. A. Klein and D. L. Hartmann, "Spurious trends in the ISCCP C2 data set," *Geophys. Res. Lett.,* vol. 20, pp. 455–458, 1993.

[30] R. B. Lee III, B. R. Barkstrom, G. L. Smith, J. E. Cooper, L. P. Kopia, and R. W. Lawrence, "The Clouds and the Earth's Radiant Energy System (CERES) sensors and preflight calibration plans," *J. Atmos. Ocean. Technol.,* vol. 13, pp. 300–313, Apr. 1996.

[31] Z. Li and H. G. Leighton, "Global climatologies of solar radiation budgets at the surface and in the atmosphere from 5 years of ERBE data," *J. Geophys. Res.,* vol. 98, no. D3, pp. 4919–4930, 1993.

[32] Z. Li, H. G. Leighton, K. Masuda, and T. Takashima, "Estimation of SW flux absorbed at the surface from TOA reflected flux—Top of atmosphere," *J. Clim.,* vol. 6, no. 2, pp. 317–330, 1993.

[33] B. Lin, B. A. Wielicki, P. Minnis, and W. Rossow, "Estimation of water cloud properties from satellite microwave and optical measurements in oceanic environments, I: Microwave brightness temperature simulations," *J. Geophys. Res.,* to be published.

[34] W. P. Menzel, D. P. Wylie, and K. L. Strabala, "Seasonal and diurnal changes in cirrus clouds as seen in four years of observations with the VAS," *J. Appl. Meteorol.,* vol. 31, pp. 370–385, 1992.

[35] P. Minnis, D. P. Garber, D. F. Young, R. F. Arduini, and Y. Takano, "Parameterizations of reflectance and effective emittance for satellite remote sensing of cloud properties," *J. Atmos. Sci.,* to be published.

[36] P. Minnis, K.-N. Liou, and D. F. Young, "Inference of cirrus cloud properties using satellite-observed visible and infrared radiances, II—Verification of theoretical radiative properties, *J. Atmos. Sci.,* vol. 50, pp. 1305–1322, 1993.

[37] J. Paden, G. L. Smith, R. B. Lee III, D. K. Pandey, and S. Thomas, "Reality check: A point response function (PRF) comparison of theory to measurements for the Clouds and the Earth's Radiant Energy System (CERES) Tropical Rainfall Measuring Mission (TRMM) instrument," in *Proc. SPIE,* Orlando, FL, 1997, vol. 3074, Paper 3074-15.

[38] R. T. Pinker and I. Laszlo, "Modeling surface solar irradiance for satellite applications on a global scale," *J. Appl. Meteorol.,* vol. 31, pp. 194–211, 1992.

[39] V. Ramanathan, B. Subasilar, G. J. Zhang, W. Conant, R. D. Cess, J. T. Kiehl, H. Grassl, and L. Shi, "Warm pool heat budget and shortwave cloud forcing—A missing physics," *Science,* vol. 267, pp. 499–503, 1995.

[40] V. Ramanathan, R. D. Cess, E. F. Harrison, P. Minnis, and B. R. Barkstrom, "Cloud-radiative forcing and climate—Results from the earth radiation budget experiment," *Science,* vol. 243, pp. 57–63, 1989.

[41] D. A. Randall, Harshvardhan, D. A. Dazlich, and T. G. Corsetti, "Interactions among radiation, convection, and large-scale dynamics in a general circulation model," *J. Atmos. Sci.,* vol. 46, pp. 1943–1970, 1989.

[42] W. Rossow, L. Garder, P. Lu, and A. Walker, "International Satellite Cloud Climatology Project (ISCCP) documentation of cloud data," *World Meteorol. Org.,* WMO/TD 266 (revised), p. 76, 1991.

[43] W. B. Rossow and L. C. Garder, "Cloud detection using satellite measurements of infrared and visible radiances for ISCCP," *J. Clim.,* vol. 6, no. 12, pp. 2341–2369, 1993.

[44] J. Schmetz, "On the parameterization of the radiative properties of broken clouds," *Tellus,* vol. 36A, pp. 417–432, 1984.

[45] G. L. Smith, R. N. Green, E. Raschke, L. M. Avis, J. T. Suttles, P. Wielicki, A. Bruce, and R. Davies, "Inversion methods for satellite studies of the Earth radiation budget: Development of algorithms for

the ERBE mission," *Rev. Geophys.,* vol. 24, pp. 407–421, 1986.
[46] G. L. Stephens and S.-C. Tsay, "On the cloud absorption anomaly," *R. Meteorol. Soc.,* vol. 116, pp. 671–704, 1990.
[47] L. L. Stowe, E. P. McClain, R. Carey, P. Pellegrino, and G. G. Gutman, "Global distribution of cloud cover derived from NOAA/AVHRR operational satellite data," *Adv. Space Res.,* vol. 11, no. 3, pp. 51–54, 1991.
[48] R. Stuhlmann, E. Raschke, and U. Schmid, "Cloud generated radiative heating from METEOSAT data," in *Proc. IRS 92: Current Problems Atmos. Rad.* Deepak, 1993, pp. 69–75.
[49] J. T. Suttles, R. N. Green, P. Minnis, G. L. Smith, W. Staylor, B. A. Wielicki, I. J. Walker, D. F. Young, V. R. Taylor, and L. L. Stowe, "Angular radiation models for the earth-atmosphere system," NASA Reference Pub. 1184, July 1988, p. 144.
[50] J. T. Suttles, B. A. Wielicki, and S. Vemury, "Top-of-atmosphere radiative fluxes—Validation of ERBE scanner inversion algorithm using nimbus-7 ERB data," *J. Appl. Meteorol.,* vol. 31, no. 7, pp. 784–796, 1992.
[51] W.-C. Wang, G.-Y. Shi, and J. T. Kiehl, "Incorporation of the thermal radiative effect of CH4, N2O, Ch2Cl2, and CFDl3 into the national center for atmospheric research community climate model," *J. Geophys. Res.,* vol. 96, pp. 9097–9103, 1991.
[52] R. M. Welch, S. K. Sengupta, A. K. Goroch, P. Rabindra, N. Rangaraj, and M. S. Navar, "Polar cloud and surface classification using AVHRR imagery—An intercomparison of methods," *J. Appl. Meteorol.,* vol. 31, no. 5, pp. 405–420, 1992.
[53] C. H. Whitlock, T. P. Charlock, W. F. Staylor, R. T. Pinker, I. Laszlo, A. Ohmura, H. Gilgen, T. Konzelman, R. C. DiPasquale, C. D. Moats, S. R. LeCroy, and N. A. Ritchey, "First global WCRP shortwave surface radiation budget dataset," *Bull. Amer. Met. Soc.,* vol. 76, pp. 905–922, 1995.
[54] B. A. Wielicki and R. N. Green, "Cloud identification for ERBE radiative flux retrieval," *J. Appl. Meteorol.,* vol. 28, no. 11, pp. 1133–1146, 1989.
[55] B. A. Wielicki, R. D. Cess, M. D. King, D. A. Randall, and E. F. Harrison, "Mission to planet Earth: Role of clouds and radiation in climate," *Bull. Amer. Meteorol. Soc.,* vol. 76, pp. 2125–2153, 1995.
[56] B. A. Wielicki, B. R. Barkstrom, E. F. Harrison, R. B. Lee III, G. L. Smith, and J. E. Cooper, "Clouds and the Earth's Radiant Energy System (CERES): An earth observing system experiment," *Bull. Amer. Meteorol. Soc.,* vol. 77, 853–868.
[57] M. L. C. Wu, and L.-P. Chang, "Longwave radiation budget parameters computed from ISCCP and HIRS2/MSU products," *J. Geophys. Res.,* vol. 97, no. D9, pp. 10083–10101, 1992.
[58] D. F. Young, P. Minnis, T. Wong, D. R. Doelling, and G. G. Gibson, "Temporal interpolation methods for the Clouds and the Earth's Radiant Energy System (CERES)," *J. Appl. Meteorol.,* to be published.
[59] D. Winker, personal communication, Feb. 1998

Bruce A. Wielicki, photograph and biography not available at the time of publication.

Bruce R. Barkstrom received the B.S. degree in physics from the University of Illinois, Urbana, and the M.S. and Ph.D. degrees in astronomy from Northwestern University, Evanston, IL.
He is a Senior Research Scientist in the Atmospheric Sciences Division, NASA Langley Research Center, Hampton, VA. He is the Principal Investigator for the CERES Instrument Investigations, and he served as the Principal Investigator of the ERBE spacecraft instruments and science investigations.

Bryan A. Baum, photograph and biography not available at the time of publication.

Thomas P. Charlock, photograph and biography not available at the time of publication.

Richard N. Green, photograph and biography not available at the time of publication.

David P. Kratz, photograph and biography not available at the time of publication.

Robert B. Lee, III received the B.S. degree in physics from Norfolk State University, Norfolk, VA, and the M.S. degree in engineering physics from the University of Virginia, Charlottesville.
He is a Senior Research Scientist in the Atmospheric Sciences Division, NASA Langley Research Center, Hampton, VA. He is a Co-Investigator on the CERES Science Team and the Leader of its Instrument Working Group. He is also a Co-Investigator on the International ScaRaB (Scanner for Radiation Budget) Science Working Group Science Team. He served as a Co-Investigator on the Earth Radiation Budget Experiment (ERBE) Science Team and Leader of its Instrument Working Group.

Patrick Minnis, photograph and biography not available at the time of publication.

G. Louis Smith is a Research Professor with the Virginia Polytechnic Institute and State University, Blacksburg. He is a Co-investigator for the CERES Science Team and a Principal Investigator on the International ScaRaB Science Working Group Science Team.

Takmeng Wong, photograph and biography not available at the time of publication.

David F. Young, photograph and biography not available at the time of publication.

Robert D. Cess, photograph and biography not available at the time of publication.

James A. Coakley, Jr., photograph and biography not available at the time of publication.

Dominique A. H. Crommelynck received the B.S. and Ph.D. degrees from the Universite Libre de Bruxelles, Brussels, Belgium.
He is a Staff Scientist at the Institut Royal Meteorologique, Brussels. He is a Principal Investigator on the International ScaRaB Science Working Group Science Team and a Co-Investigator on the CERES Science Team. He is the Principal Investigator for the Solar Constant (SOLCON) experiment on Spacelab 1/Space Shuttle, the Solar Variations (SOVA) experiment on the EURECA spacecraft, and the VIRGO experiment on the SOHO spacecraft.

Leo Donner, photograph and biography not available at the time of publication.

Veerabhadran Ramanathan, photograph and biography not available at the time of publication.

Robert Kandel, photograph and biography not available at the time of publication.

David A. Randall, photograph and biography not available at the time of publication.

Michael D. King, photograph and biography not available at the time of publication.

Larry L. Stowe, photograph and biography not available at the time of publication.

Alvin J. Miller, photograph and biography not available at the time of publication.

Ronald M. Welch, photograph and biography not available at the time of publication.